Deregulated BCL6 expression recapitulates the pathogenesis of human diffuse large B cell lymphomas in mice

Giorgio Cattoretti,[1,2,5] Laura Pasqualucci,[1,2,5] Gianna Ballon,[1,4] Wayne Tam,[1,4] Subhadra V. Nandula,[2] Qiong Shen,[1] Tongwei Mo,[1] Vundavalli V. Murty,[1,2] and Riccardo Dalla-Favera[1,2,3,*]

[1]Institute for Cancer Genetics, Columbia University, New York, New York 10032
[2]Department of Pathology, Columbia University, New York, New York 10032
[3]Department of Genetics & Development, Columbia University, New York, New York 10032
[4]Present address: Department of Pathology & Laboratory Medicine, Weill Medical College of Cornell University, New York, New York 10021
[5]These authors contributed equally to this work.
*Correspondence: rd10@columbia.edu

Summary

Diffuse large B cell lymphomas (DLBCL) derive from germinal center (GC) B cells and display chromosomal alterations deregulating the expression of BCL6, a transcriptional repressor required for GC formation. To investigate the role of BCL6 in DLBCL pathogenesis, we have engineered mice that express BCL6 constitutively in B cells by mimicking a chromosomal translocation found in human DLBCL. These mice display increased GC formation and perturbed post-GC differentiation characterized by a decreased number of post-isotype switch plasma cells. Subsequently, these mice develop a lymphoproliferative syndrome that culminates with the development of lymphomas displaying features typical of human DLBCL. These results define the oncogenic role of BCL6 in the pathogenesis of DLBCL and provide a faithful mouse model of this common disease.

Introduction

The *BCL6* proto-oncogene encodes a transcriptional repressor required for the formation of germinal centers (GC) (Ye et al., 1993a; Ye et al., 1997; Dent et al., 1997), the structures in which mature B cells undergo somatic hypermutation (SHM) of their immunoglobulin variable region (IgV) genes and Ig class-switch recombination (CSR) before being selected based on the production of antibodies with high affinity for the antigen (Rajewsky, 1996). GCs are required for antibody-mediated immune responses and are also important in pathology, since GC B cells are thought to represent the cell of origin of most types of human B cell lymphomas (Dalla-Favera and Gaidano, 2001; Küppers et al., 1999). *BCL6*-deficient mice display normal B cell development except for their inability to form GC (Dent et al., 1997; Ye et al., 1997), consistent with the fact that, within the B cell lineage, BCL6 is expressed only in the GC (Cattoretti et al., 1995). BCL6 exerts its transcriptional repressor function by binding to specific DNA sequences via its C-terminal zinc finger domain and recruiting corepressor complexes through two noncontiguous domains, a N-terminal POZ domain and a second, less characterized domain in the middle portion of the molecule (Chang et al., 1996; Seyfert et al., 1996).

The biologic function of BCL6 in the GC is presumably to favor the sustained proliferation of B cells involved in GC formation by modulating the transcription of genes involved in cell activation, differentiation, and cell cycle arrest (Shaffer et al., 2000; Niu et al., 2003; Tunyaplin et al., 2004). In addition, BCL6 binds the promoter region of the p53 tumor suppressor gene and suppresses its transcription in GC B cells, perhaps as a means to allow the DNA breaks necessary for SHM and CSR to occur without eliciting a p53-mediated apoptotic response (Phan and Dalla-Favera, 2004). BCL6 expression is regulated by signals involved in the control of GC development, including T cell-induced CD40 signaling, which downregulates BCL6 at the transcriptional level, and antigen-induced B cell receptor (BCR) signaling, which leads to BCL6 degradation by the ubiquitin-proteasome pathway (Niu et al., 1998; Niu et al., 2003). BCL6 activity is also regulated by acetylation, which inactivates its transrepressive function by preventing the recruitment of corepressor complexes (Bereshchenko et al., 2002; Fujita et al., 2004). Post-GC B cells lack BCL6 expression, and downregulation of its function is thought to be necessary for the differentiation of B cells into plasma cells and memory B cells.

SIGNIFICANCE

Diffuse large B cell lymphoma (DLBCL), the most common type of human B cell lymphoma, is poorly understood in its pathogenesis and is incurable in a subset of cases. This is partly due to lack of knowledge about the role of *BCL6*, the gene that is most frequently altered in DLBCL, and to the absence of animal models that recapitulate both the genetics and the biology of the disease. Here we have engineered a mouse model of DLBCL that shows the specific role of BCL6 in its pathogenesis and displays most of the critical features of the corresponding human tumor. This model can be used to test novel therapies targeted to BCL6.

The *BCL6* proto-oncogene was originally identified because of its involvement in 3q27 chromosomal translocations, which are found in ~40% of cases of diffuse large B cell lymphoma (DLBCL) and in 5%–10% of cases of follicular lymphoma (FL) (Ye et al., 1993a; Ye et al., 1993b; Kerckaert et al., 1993; Lo Coco et al., 1994). These translocations place an intact *BCL6* coding domain under the influence of heterologous promoter regions derived from a variety of alternative partner chromosomes (>20), including the immunoglobulin heavy (H) and light (L) chain genes (Ye et al., 1995; Chen et al., 1998; Pasqualucci et al., 2003a). Since these promoters allow for a broader pattern of expression throughout B cell development than the natural *BCL6* promoter, the translocation results in deregulated expression of the normal BCL6 protein. In addition, the 5′ noncoding region of *BCL6* is targeted by SHM in normal GC B cells as well as in GC-derived malignancies (Migliazza et al., 1995; Pasqualucci et al., 1998; Shen et al., 1998; Peng et al., 1999; Capello et al., 2000). While the functional significance of most *BCL6* somatic mutations remains unknown, in 13% of DLBCLs (but not in normal GC B cells), these were found to disrupt the negative autoregulatory circuit that normally controls BCL6 expression by altering two BCL6 binding sites within the first noncoding exon of the gene (Pasqualucci et al., 2003b; Wang et al., 2002). Collectively, translocations and exon1 mutations are observed in ~50% of DLBCL cases, where they are thought to prevent the downregulation of BCL6 expression that is normally associated with differentiation into post-GC B cells. However, direct experimental evidence implicating BCL6 in DLBCL pathogenesis is still lacking.

To directly test the role of deregulated BCL6 in DLBCL pathogenesis, we have engineered mice to express a murine BCL6 coding domain under the control of the immunoglobulin Iμ promoter, thereby recapitulating the outcome of one of the translocations associated with human DLBCL. Our results demonstrate a direct role for BCL6 in DLBCL development and provide a model to study the biology of this disease and to test novel therapeutic approaches.

Results

Construction of mice expressing deregulated BCL6

To obtain deregulated BCL6 expression in mouse B cells in vivo, we used homologous recombination to insert a HA-tagged, full-length murine BCL6 coding sequence downstream of the immunoglobulin heavy chain (IgH) Iμ promoter on mouse chromosome 12 in murine ES cells. The recombinant locus can produce a chimeric mRNA (Iμ-HABCL6) whose transcription is driven by the Iμ promoter, which is normally active in mature B cells (Lennon and Perry, 1985), thereby mimicking one of the chromosomal translocations, t(3;14)(q27;q32), occurring in human DLBCLs (Figure 1A) (Ye et al., 1995). Three independent mouse lines were generated (4E12, 5H7, 4B8); in all of them, mice heterozygous or homozygous for the manipulated allele were born as expected for Mendelian transmission (Figure 1B and data not shown), and were indistinguishable at birth from their wt littermates. IμHABCL6 mice were fertile, showed no gross developmental abnormalities in all organs analyzed, and displayed a normal B cell repertoire (not shown).

Northern blot analysis of mice between 8 and 12 weeks of age after immunization with sheep red blood cells (SRBC) documented the presence of a transcript corresponding to the size predicted for the knockin allele in purified splenic CD19$^+$ cells from the IμHABCL6 mice, but not in other tissues or in wt littermates (Figure 2A, left panel). Accordingly, Western blot analysis with an anti-HA antibody, which can detect only the exogenous tagged BCL6 protein, revealed a specific band exclusively in the IμHABCL6 splenic CD19$^+$ B cell population (Figure 2A, right panel). Both exogenous and endogenous proteins were recognized by the anti-BCL6 antibodies, which showed BCL6 positivity in thymus and CD19$^+$ B cells from both wt and IμHABCL6 mice, as expected.

We then characterized the topological distribution of BCL6 expression by immunohistochemistry (IHC) using antibodies recognizing the exogenous (anti-HA) or both the endogenous and exogenous (anti-BCL6) BCL6 protein. After immunization with SRBC, both IμHABCL6 and wt littermates formed BCL6-positive GCs surrounded by mantle zone and marginal zone B cells in which BCL6 is not detectable by IHC. However, a number of strongly BCL6-positive cells were also detected outside the GC in the IμHABCL6 mice, but not in control mice (Figure 2B, top panels). Staining for HA and PNA (a GC marker, not shown) demonstrated expression of the exogenous protein within—as well as outside—the GC of IμHABCL6 mice (Figure 2B, bottom panels). These cells, which were not observed in wt animals, represented differentiated plasma cells, as demonstrated unambiguously by their morphologic features, coexpression of the specific marker CD138, and production of cytoplasmic heavy chain immunoglobulins of all isotypes (see Figures 2C–2E for representative data; note that double IHC analysis with other plasma cell markers such as BLIMP-1 and XBP-1 [Lin et al., 2003] is not technically feasible with currently available reagents). Deregulated expression of BCL6 in plasma cells was further documented by double IHC and double immunofluorescence staining of the intestinal lamina propria—where these cells localize in large numbers—using CD138/BCL6, CD138/HA, and cytoplasmic IgA/BCL6 or IgG1/BCL6 antibodies (Figures 2C–2E). However, it was noted that only a fraction (~15%) of plasma cells expressed BCL6 at high levels; this may be due to the nonhomogeneous activity of the Iμ promoter in plasma cells as well as to recombination events (deletions and mutations) occurring in the region 5′ of the switch μ sequences, which may affect BCL6 expression (Stavnezer et al., 1985; Li et al., 1994). Together, these data showed that exogenous BCL6 was detectable in both the GC and plasma cells of IμHABCL6 mice, indicating its transcriptional deregulation.

Deregulated expression of BCL6 leads to increased GC formation and perturbed plasmacytoid differentiation

Young (<5 month), immunologically mature IμHABCL6 mice displayed a normal number and distribution of B and T cells and a normal architecture of all lymphoid organs, including thymus, spleen, lymph nodes, and gut-associated lymphoid tissue. However, the same mice displayed a small (20%–50%), but significant, reduction in total serum immunoglobulin levels of all subclasses—except for IgM—both under basal conditions and after immunization with T-dependent antigens (NP) (Supplemental Figures S1A and S1B). Despite these defects, affinity maturation appeared normal (Supplemental Figure S1C), suggesting that SHM was unaffected. IμHABCL6 mice displayed also a ~30% reduction in the number of total plasmacytoid cells (B220$^{+/-}$ CD138$^+$), mainly due to a decrease in

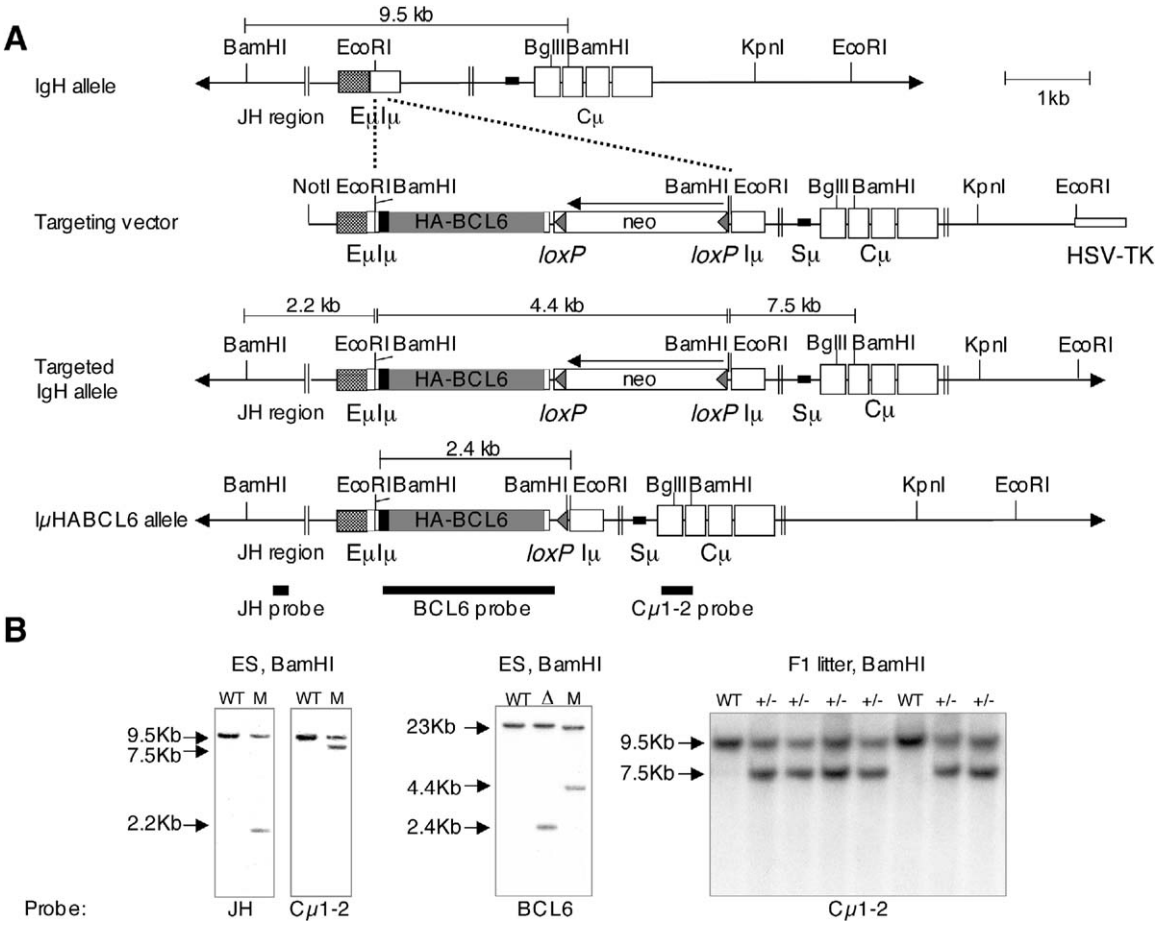

Figure 1. Generation of IμHABCL6 knockin mice

A: Targeting strategy. The murine germline Ig heavy chain (IgH) locus is shown before (top scheme) and after (middle scheme) homologous recombination with the targeting vector, which contains a murine BCL6 cDNA downstream and in frame with a hemagglutinin (HA) tag, a neomycin-resistance (neo) gene under the control of the PGK promoter and flanked by two *loxP* sites, and the thymidine kinase gene (HSV-TK) for positive selection of the transfected cells. The final configuration of the recombined allele after cre-mediated excision of the neo cassette in vitro is shown at the bottom. Expected restriction fragments and probes used for Southern blotting are also indicated. Eμ, immunoglobulin heavy chain intronic enhancer; Iμ, immunoglobulin mu sterile transcript promoter; Cμ, the four Cμ exons; Sμ, switch mu region.

B: Southern blot analysis of BamHI-digested ES cells DNA from wild-type (wt) and homologous recombinant clones before (M) and after (Δ) Cre mediated recombination. On the right, BamHI-digested tail DNA from F1 offspring.

post-CSR plasma cells (IgM^-IgD^-), while IgM^+IgD^+ plasma cells are normal (Supplemental Figure S2). These findings indicate that deregulated BCL6 expression is compatible with normal CSR and plasmacytoid differentiation, although it favors the production of IgM-secreting plasma cells (see Discussion).

We then evaluated the GC responses (size and number of GC) of IμHABCL6 and wt littermates by flow cytometric analysis of PNA expression and in situ IHC staining for PNA/BCL6 on spleens obtained from mice before and after immunization with SRBC. As expected, unimmunized wt mice displayed a very limited number of scarcely developed GCs that increased significantly upon immunization (Figure 3A). Notably, nonimmunized IμHABCL6 mice displayed an increased number of GCs, comparable to that observed upon immunization of wt mice (compare the second and third bars from left in Figure 3A). This significant increase in the number of GCs as well as in the total GC area persisted when animals were examined 10 days after immunization (bars 3 and 4 from left in Figures 3A and 3B), and was comparable to that observed in immunized $AID^{-/-}$ mice, which were used as control as they are known to form enlarged GCs (Muramatsu et al., 2000) (data not shown). However, the sizes of GCs were not notably different in IμHABCL6 versus control mice, in contrast to those of $AID^{-/-}$ mice. The analysis of proliferating (BrdU) or apoptotic (Annexin-V^+) B cells indicated that the increased number of GCs in IμHABCL6 mice was not associated with changes in the fraction of proliferating or dying B cells within the GC (data not shown). Overall, these data suggest that deregulated BCL6 expression increases the number of GCs by lowering the threshold for B cells to enter the GC reaction.

To gain further insight into the mechanism of increased GC formation, we constructed mice expressing exclusively the IμHABCL6 allele in the absence of endogenous BCL6 alleles. To this end, we bred the IμHABCL6 allele into $BCL6^{-/-}$ mice,

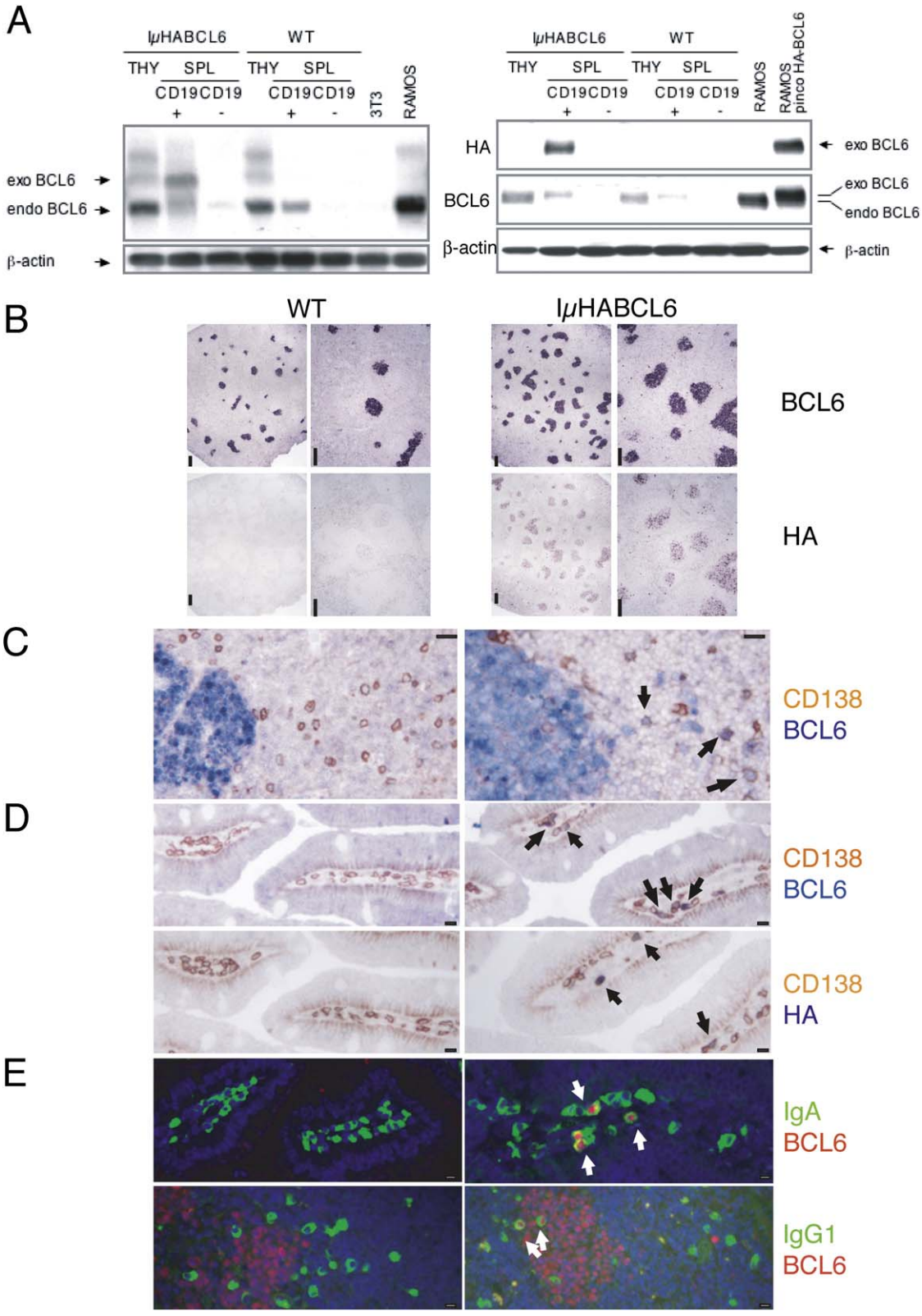

Figure 2. Expression of the HABCL6 protein in IμHABCL6 mice

A: Northern (left) and Western (right) blot analysis for BCL6 expression in thymus, $CD19^+$, and $CD19^-$ splenic cells purified from IμHABCL6 mice and wild-type (wt) littermates. A BCL6 cDNA probe detected endogenous BCL6 mRNA in thymus and $CD19^+$ B cells of both wt and knockin mice, as expected. A band corresponding to the size of the exogenous mRNA transcript is detected only in $CD19^+$ cells of the knockin mice. An analogous pattern of expression is observed by WB analysis using anti-HA (exogenous) and anti-BCL6 (exogenous+endogenous) antibodies on the same cell populations. Ramos cells stably transduced with a HA-BCL6 retroviral vector are shown as control. β-actin monitors the loading.

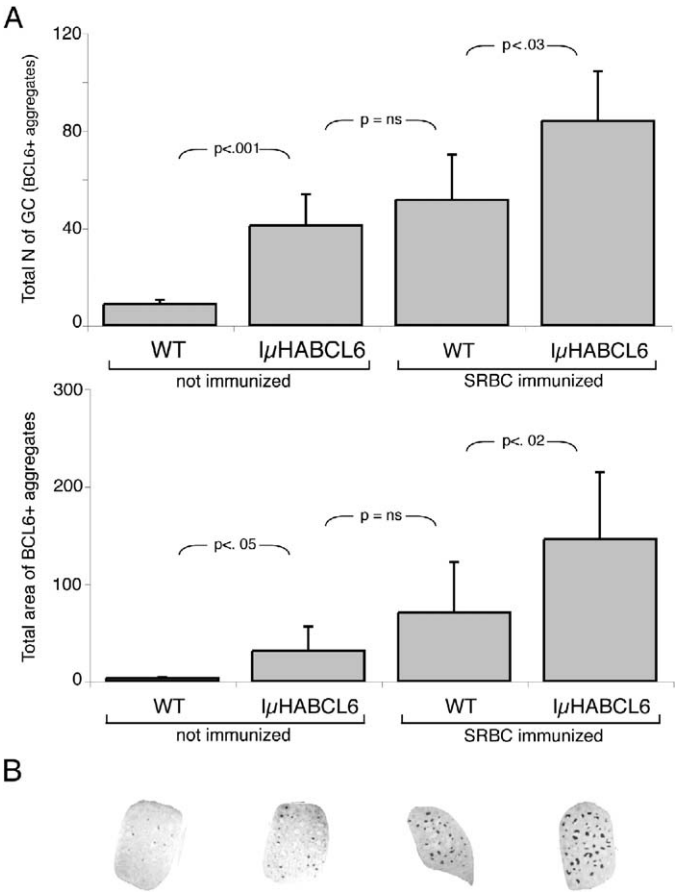

Figure 3. Increased GC formation in IμHABCL6 mice

A: The total number of GCs before and after SRBC immunization was estimated in spleen sections from wt and IμHABCL6 littermates stained with anti-BCL6 and anti-PNA antibodies, and normalized to the total spleen area analyzed (top). The ImageJ software (RSB, NIH, Washington, DC) was used to determine the total area of GCs, defined as BCL6 positive aggregates and expressed as Kpixels (1,000 pixels) (bottom). Error bars indicate standard deviations.

B: BCL6 staining of representative spleen sections from the mice indicated in **A**.

which lack GCs (Ye et al., 1997; Dent et al., 1997). Analysis of lymphoid organs upon SRBC immunization showed that expression of the exogenous HABCL6 protein in IμHABCL6/BCL6$^{-/-}$ mice was sufficient to induce the proliferation of B cells, as documented by the appearance of a substantial number of cells expressing the proliferation marker Ki67 (Figure 4, top panels). These cells also coexpress the GC-associated marker PNA, suggesting that they represent bona fide GC B cells (Figure 4, bottom panels). However, these cells did not aggregate in typical GC structures, most likely because BCL6 is needed in other non-B cells necessary for GC formation (Ye et al., 1997; Dent et al., 1997). The IμHABCL6 knockin allele was unable to rescue the inflammatory phenotype of BCL6$^{-/-}$ mice (Ye et al., 1997; Dent et al., 1997), also in keeping with its absence from T cells and antigen presenting cells (not shown). These results suggest that one effect of deregulated BCL6 expression is to allow a proliferative GC phenotype in B cells.

Early benign lymphoproliferative disease in IμHABCL6 mice

When sacrificed at 6 months of age, a modest splenomegaly was noted in a fraction (4/24, 17%) of IμHABCL6 mice. Microscopic analysis showed evidence for abnormal B cell expansions involving predominantly the spleen, but also the lymph nodes, in all three lines (overall, 10/24 [42%] IμHABCL6 animals versus 2/18 [11%] wt controls; range = 33 to 83% in the 3 lines). These abnormalities were represented by a partial effacement of the follicular architecture with the appearance of blast cells (Figure 5, second panel from left). Immunostaining of spleen populations indicated that the expanded white pulp zones were composed predominantly of B cells, but also included disorganized accumulations of other cell types such as T cells and dendritic cells. These abnormal expansions were polyclonal/oligoclonal upon analysis of their rearranged endogenous Ig genes (see below), and displayed a normal karyotype (data not shown). Taken together, these features are compatible with a diagnosis of benign lymphoproliferative disease (LPD). In addition, 4 of the 24 (17%) IμHABCL6 mice analyzed at this age displayed a complete effacement of the splenic lymphoid architecture due to the proliferation of large lymphoid cells, consistent with a diagnosis of DLBCL (see below). The B cell population enriched in the LPD (IgM^{high}-IgD^{low} B cells, which are negative for both CD23 and CD21) appears to be predominant in some DLBCL (compare second and third panels from left in Supplemental Figure S3B), suggesting that it may be progressively selected during tumorigenesis. Overall, these morphological and phenotypic criteria, together with the temporal evolution toward clonality, suggest that the LPD may represent a stage toward the development of DLBCL (see Discussion).

Development of DLBCL in IμHABCL6 mice

Starting at approximately 13 months of age, IμHABCL6 mice showed increased mortality, such that only ~80% of the animals survived at 15 months (p value < 0.01) (Figure 6A). Histologic examination of 79 knockin mice and 84 wt littermates between 15 and 20 months of age revealed that 36% (5H7 line) to 62% (4E12 line) of the animals had developed clonal B cell lymphomas, predominantly of splenic origin, with or without nodal involvement (Figure 6B). These tumors displayed a mature B cell phenotype (IgM$^+$IgD$^+$CD43$^-$), and most were histologically reminiscent of the human DLBCL (75% of cases), with a minority of non-DLBCL lymphomas (not shown). BCL6 ex-

B: Serial spleen sections of SRBC-immunized wt and IμHABCL6 knockin mice stained with anti-BCL6 (top) and anti-HA (bottom) antibodies. For each genotype, images are shown at low (scale bar 40 μm, left panel) and high (scale bar 10 μm, right panel) magnification.

C: Double immunostaining of spleen sections from wt and IμHABCL6 mice with BCL6 (blue) and the plasma cell marker CD138 (brown) (scale bar 5 μm).

D–E: Double immunostaining of gut sections (Peyer's patches) from wt (left) and IμHABCL6 (right) animals, with markers color-coded as indicated along the right side: CD138/BCL6 (**D**, top), CD138/HA (**D**, bottom), BCL6/IgA (**E**, top), and BCL6/IgG1 (**E**, bottom) (scale bar 1 μm).

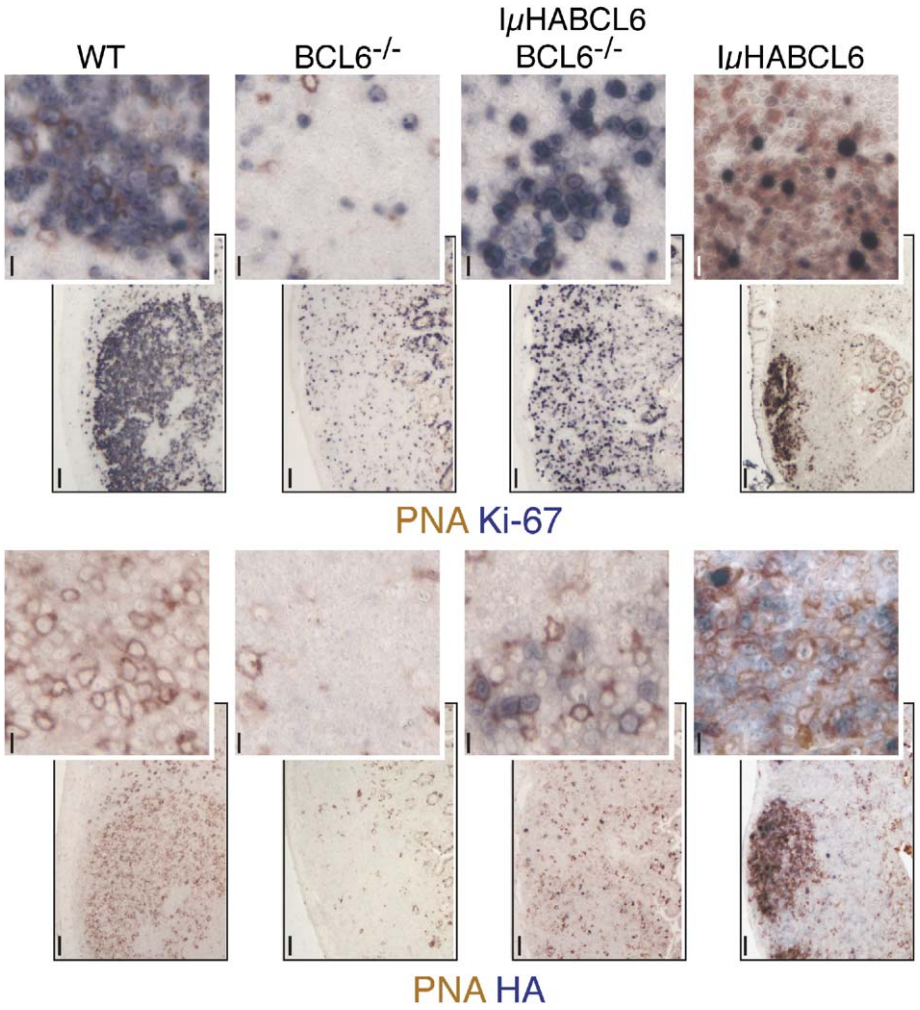

Figure 4. Introduction of the IμHABCL6 allele in a BCL6-deficient background results in reappearance of proliferating B cells with GC phenotype

Serial sections of Peyer's patches from wt, $BCL6^{-/-}$, $BCL6^{-/-}$/IμHABCL6, and IμHABCL6 mice immunized with SRBC. Top panels: double immunostaining with PNA (brown) and the proliferation marker Ki67 (blue) (scale bar 10 μm, inset 1 μm). Bottom panels: double immunostaining with PNA and HA (scale bar 10 μm, inset 1 μm).

pression in these tumors was heterogeneous, ranging from high expression detectable by IHC (Figure 5, right panel) to levels below detectability by IHC. Notably, molecular analysis of the rearranged IgV genes from eleven lymphoma biopsies confirmed their clonal derivation (Figure 6C) and revealed the presence of somatic mutations in 9/11 (82%) cases studied (Supplemental Table S1), indicating that these tumors have transited through the GC. Additional IHC and flow cytometric analysis indicated that these tumors express IgM in most of the cases, lack the plasmacytoid marker CD138, and have variable expression of MUM1/IRF4 (Supplemental Figure S3A), a marker identifying a subset of late and activated GC centrocytes in humans (Falini et al., 2000). Overall, this phenotype is consistent with a GC derivation, with variable expression of late GC markers, analogous to a large fraction of human DLBCL (see Discussion). Spectral karyotype (SKY) analysis revealed complex nonrandom cytogenetic abnormalities in 14/16 tumors analyzed, including 13 DLBCLs and one marginal zone lymphoma (Supplemental Table S2). These clonal karyotypic aberrations comprised both numerical and structural aberrations, and in most cases (13/14) involved chromosome 15, either by trisomy (n = 12) or by translocation (t[12;15] in one case, both spleen and thymus) (Figure 6D). Trisomy of chromosome 13 was the second most frequent abnormality, with 7/14 positive cases, and was recurrently seen in association with trisomy 15.

In summary, analysis of the three independent IμHABCL6 lines uncovered alterations in B cell proliferation (LPD and/or lymphoma) by the age of 20 months in 76%–89% of mice. In contrast, a very low background incidence of lymphomas was observed in wt littermates (Figure 6B).

Discussion

Implications for the biological functions of BCL6

In vitro studies indicate that BCL6 maintains the GC phenotype of B cells by preventing premature cell cycle arrest, differentiation, and death (Shaffer et al., 2000; Niu et al., 2003; Tunyaplin et al., 2004). The results herein suggest that BCL6 may also be involved in the establishment of the GC reaction. The observation that nonimmunized mice expressing deregulated BCL6 can form GCs in numbers comparable to those observed in wt mice upon immunization (Figure 3A) suggests that BCL6 may control the threshold allowing B cells to enter GC formation. Specifically, BCL6 appears to lower the threshold for B cells to enter the cell cycle, since B cell-restricted expression of BCL6

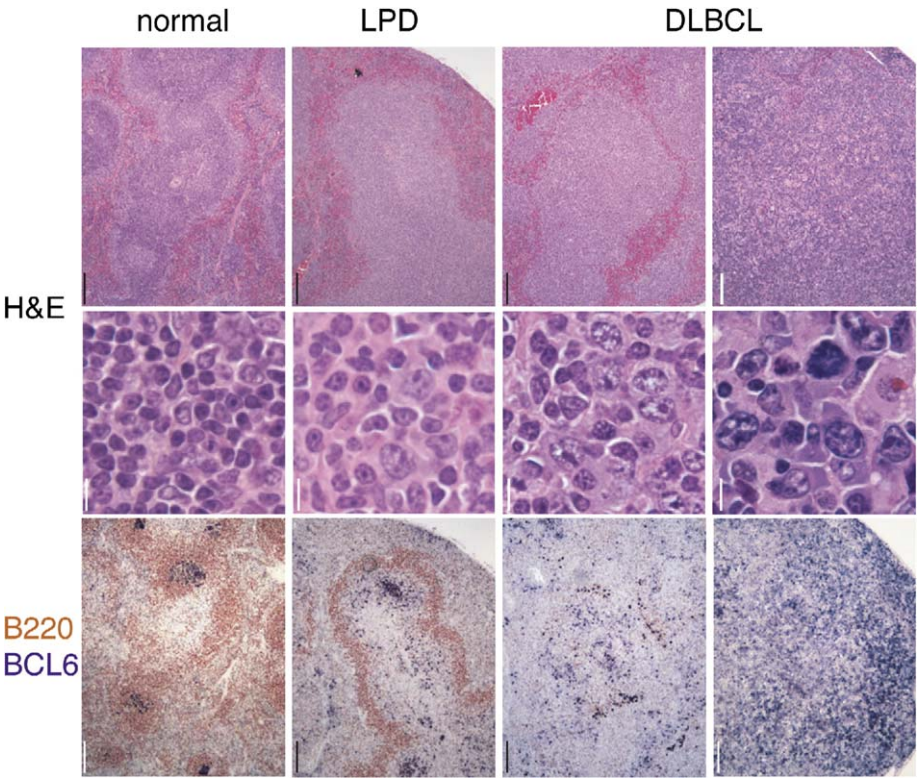

Figure 5. Development of LPD and DLBCL in IμHABCL6 mice

Spleen sections of wt (left) and IμHABCL6 mice displaying LPD (middle) or overt DLBCL (right two panels) were stained with H&E or double immunostained with BCL6 (blue) and B220 (brown) as indicated (top and bottom panels, scale bar 10 μm; middle panels, scale bar 1 μm).

in otherwise BCL6 null mice leads to the reappearance of proliferating B cells with GC markers upon immunization (Figure 4). This notion is also consistent with the observation that B cells expressing an inactive BCL6 molecule, i.e., a truncated *BCL6* allele lacking 4 of the 6 zinc finger DNA binding domains and incapable of nuclear localization and DNA binding, remain alive and quiescent in vivo (Ye et al., 1997). Recent data imply that BCL6 may favor proliferation by directly inhibiting the transcription of the cell cycle arrest genes p53 and p21 (Phan and Dalla-Favera, 2004, and unpublished data). Together, these observations suggest that the biologic function of BCL6 may be to promote GC formation by ensuring that signals such as those from the antigen and the CD40 receptor, which can alternatively induce proliferation, differentiation, or death, are licensed only for proliferation.

The results shown here also have specific implications for the role of BCL6 in controlling the differentiation of B cells to plasma cells. Based on in vitro data, it has been proposed that BCL6 expression blocks plasma cell differentiation and that this may occur via transcriptional repression of the BLIMP1 gene, which encodes a transcription factor required for the generation of all types of plasma cells (Reljic et al., 2000; Shaffer et al., 2002; Tunyaplin et al., 2004). Indeed, it was shown recently that constitutive BCL6 expression can reprogram the phenotype of plasma cells toward B cells in cell lines in vitro (Fujita et al., 2004). However, the phenotype of IμHABCL6 mice suggests that the relationship between BCL6 expression and plasma cell differentiation may be more complex in vivo. These mice have a normal number of morphologically and immunophenotypically ($CD138^+$) normal IgM^+ plasma cells, which secrete normal levels of immunoglobulins. This result suggests that constitutive BCL6 expression is compatible with plasma cell differentiation in vivo. However, the number of post-CSR plasma cells and both the basal and postimmunization serum levels of most Ig isotypes—except IgM—are slightly decreased in these mice. These alterations can be attributed at least in part to the modulatory activity of BCL6 on switching to various Ig isotypes via transcriptional repression of the sterile transcripts required for CSR (Harris et al., 1999). However, it remains possible that BCL6 inhibits isotype-switched plasma cell differentiation, and that the presence of plasma cells in IμHABCL6 mice reflects nonubiquitous activity of the Iμ promoter, leading to an escape toward plasmacytoid differentiation by B cells lacking HABCL6 expression. In conclusion, while our results seem to exclude a general role for BCL6 in inhibiting plasma cell differentiation in vivo, its role in controlling the generation of isotype-switched plasma cells remains to be further elucidated.

Implications for the role of deregulated BCL6 in DLBCL pathogenesis

The spontaneous, high-penetrance development of B cell-derived lymphoproliferations in IμHABCL6 mice defines BCL6 as an oncogene capable of inducing B cell lymphomas in vivo. A recent report described BCL6 transgenic mice that develop lymphomas, appearing at significant frequency only upon treatment with mutagens and mostly derived from T cells (Baron et al., 2004). It is likely that the phenotype of our mice better recapitulates human BCL6-mediated neoplasia due to the different strategy applied to achieve deregulated BCL6 expression. In particular, with the "knockin" approach described here, we sought to reproduce the specific structural and regulatory

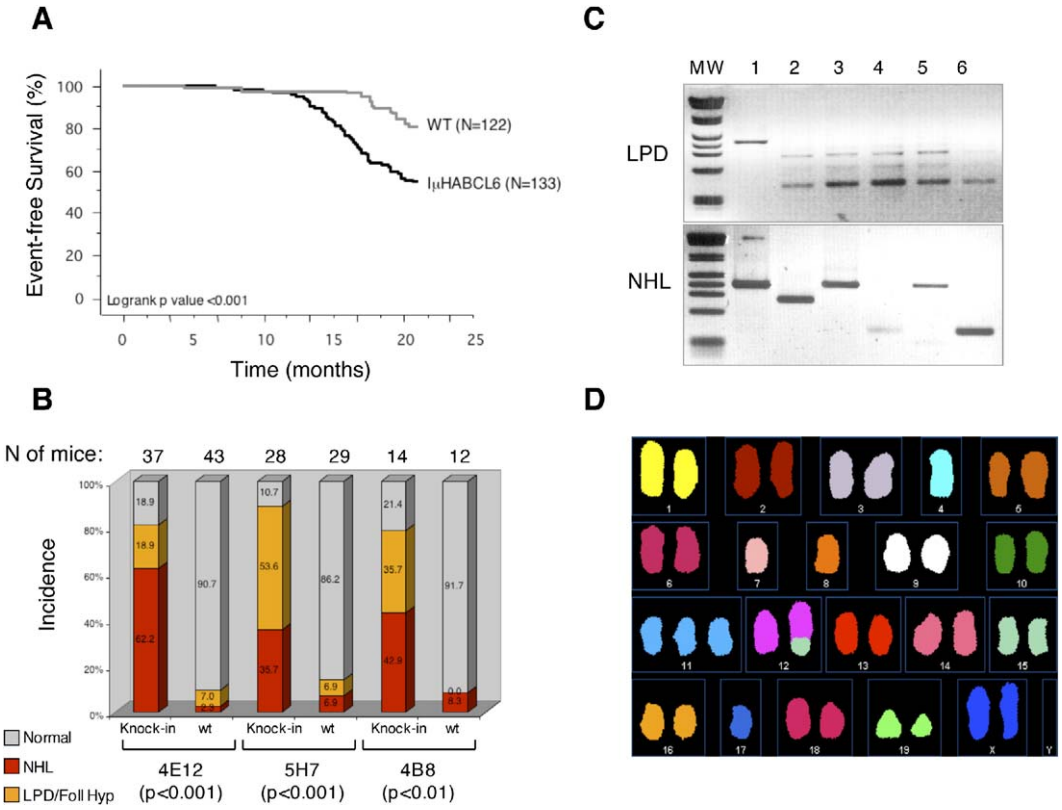

Figure 6. Characteristics of DLBCL in IμHABCL6 mice

A: Kaplan-Meyer event-free survival in IμHABCL6 mice and wt littermates.

B: Incidence of B-NHL (red) and LPD (orange) in three IμHABCL6 lines (4E12, 5H7, and 4B8) at 15–18 months of age, as compared to their wt littermates. The total number of mice analyzed in each group is indicated. Statistical analysis was performed using the χ^2 test, and the corresponding p values are given in brackets (see also Experimental Procedures).

C: IgV gene amplification from representative samples diagnosed as LPD (top gel, lanes 2–6) or DLBCL (bottom gel, lanes 1–6). MW, molecular weight marker; a clonal tumor population was loaded as control on lane 1 of the top gel. While three major bands, indicative of polyclonal rearrangements (see Experimental Procedures), are visible in each LPD sample, a single PCR product could be amplified from the DLBCL samples, each showing a discrete size and confirmed to be monoclonal by sequencing analysis.

D: SKY analysis on metaphase spread from tumor cells of IμHABCL6 mouse 4B8-22, carrying a DLBCL; a chromosomal translocation involving chromosomes 12 and 15 and a trisomy of chromosome 11 are shown.

features that characterize one of the chromosomal translocations observed in human DLBCL. Our results clearly indicate that BCL6 deregulation in mice can elicit B cell tumors resembling human DLBCL, even in the absence of exogenous mutagens.

The natural history of neoplastic progression observed in IμHABCL6 mice suggests that tumor development proceeds in at least two definable stages. The poly/oligoclonal, karyotypically normal LPD that develops early in life may represent a premalignant condition that precedes DLBCL formation. This hypothesis is supported by the temporal relationship between these two pathologic entities, as well as by morphological and phenotypic criteria (see Results). The pathological picture of LPD is complex, and has not been described so far in humans. This picture does not resemble follicular lymphoma, consistent with the notion that BCL6 deregulation in humans is associated predominantly with the de novo form of DLBCL, as opposed to the form of DLBCL that derives from follicular lymphoma (Dalla-Favera and Gaidano, 2001).

The kinetics of DLBCL formation and the clonality of the developing tumors indicate that, analogous to most tumor models, a single oncogenic hit is not sufficient for lymphomagenesis, and that deregulation of BCL6 needs to be complemented by additional genetic or epigenetic factors. Interestingly, repeated injections over the animal lifetime with potent polyclonal antigenic stimuli (SRBC; see Experimental Procedures) did not influence LPD or DLBCL development (data not shown), suggesting that chronic/repeated antigenic stimulation, an often-discussed factor in various types of human lymphoid malignancies, may not play a significant role in DLBCL pathogenesis. Conversely, the recurrent association with specific chromosomal abnormalities in murine DLBCL, such as trisomy 15 and trisomy 13, suggests that tumor progression occurs mostly through the accumulation of additional genetic lesions. The precise consequences of these whole-chromosome trisomies are not clear; however, trisomy 15—a commonly observed abnormality in murine B cell lymphomas—does not appear to target cMYC, whose expression was found to be heterogeneous and not significantly higher in DLBCL carrying this lesion (data not shown). Also, the pres-

ence of reciprocal chromosomal translocations suggests that, analogous to human DLBCL, some of these lesions may arise from mistakes in the Ig remodeling mechanisms (CSR and SHM) that normally occur within the GC (Küppers and Dalla-Favera, 2001). It has been recently reported that BCL6 suppresses p53-dependent responses to DNA breaks within the GC, thus allowing GC cells to tolerate the physiologic DNA breaks associated with CSR and SHM (Phan and Dalla-Favera, 2004). Thus, deregulated BCL6 expression may exert its oncogenic functions directly, by favoring constitutive proliferation and increased GC entry, as well as indirectly, by maintaining an increased number of B cells in a p53-negative, recombination-permissive GC environment.

A mouse model of DLBCL

Mouse models that precisely recapitulate the genetics and biology of human cancers represent much-needed tools for pathogenetic studies and for preclinical therapeutic testing. While numerous mouse models of B cell lymphoma exist, most of them have been obtained by introducing genetic lesions that are not found in human tumors and exert their oncogenic activity in immature B cells as opposed to GC B cells, the normal counterpart of most human B cell lymphomas (Dalla-Favera and Gaidano, 2001; Küppers et al., 1999). In particular, only two models of GC-derived lymphomas resembling DLBCL are available, obtained by deregulating *TCL1* and by deleting *BAD*, respectively (Hoyer et al., 2002; Ranger et al., 2003). However, neither of these two models recapitulates the genetics, and therefore possibly the biology, of human DLBCL, since the *TCL1* and *BAD* genes are not primarily altered in human DLBCL. In contrast, IμHABCL6 mice represent credible models of human DLBCL because: (1) they have been generated by transcriptional deregulation of BCL6, mimicking the outcome of the genetic lesion most commonly associated with DLBCL, (2) deregulation was achieved using the same promoter found to be juxtaposed to BCL6 in a recurrent DLBCL-associated chromosomal translocation, and (3) the resultant tumors display morphologic and immunophenotypic features typical of human DLBCL—most notably, they derive from the GC, as unequivocally demonstrated by the presence of hypermutated IgV genes. As faithful models of human DLBCLs, IμHABCL6 mice will be useful for studying the pathogenesis of this common tumor, including its early stages that go undetected in humans but can be analyzed at the LPD stage in mice. Given the increasing evidence that BCL6 represents a therapeutically targetable molecule (Bereshchenko et al., 2002; Polo et al., 2004), these mice are likely to constitute valuable preclinical models for the testing of novel therapeutic regimens specific for DLBCL.

Experimental procedures

Targeting vector construction and generation of IμHABCL6 knockin mice

The IμHABCL6 targeting vector was constructed in multiple steps by subcloning a HA-tagged murine BCL6 cassette into the pPNT vector, downstream of the IgH Iμ promoter (1.1Kb PCR fragment) and 5′ to a *loxP*-flanked stop cassette containing a neomycin-resistance gene (neo^R). A ~10 Kb EcoRI fragment including the four Cμ exons was then isolated from pEco1.1Cμ vector (gift of F. Alt, Harvard Medical School, Boston, MA) and subcloned downstream to the neo^R cassette. The targeting vector was electroporated in the embryonic stem (ES) cell line Sv129, and Neo-resistant, homologous recombinant clones were identified by Southern blot analysis of BamHI-digested DNA, using 5′ (JH) and 3′ (Cμ1-2) probes; hybridization with a Neo probe confirmed that only one recombination event had occurred. After Cre mediated excision of the neo^R cassette in vitro by transient transfection of a Cre-expressing plasmid, homologous recombinant ES cell clones were injected into blastocysts from C57BL/6 mice. Chimeric mice obtained from 3 independent ES clones transmitted the knockin allele through the germline and were all backcrossed onto a C57BL/6 background (1–8 generations) to generate lines 4E12, 5H7, and 4B8. Mice were genotyped by Southern blot analysis of BamHI-digested genomic DNA using the 3′ probe or by PCR analysis using oligonucleotides 5′HA (5′-ATG GCC TAC CCA TAC GAC GTC-3′) and mBCL6-473c (5′-TGA ACT TCC TGC ATG TGT CGA-3′).

Tumor-free survival and statistical analysis

Mice were housed and sacrificed according to the regulations of the Department of Veterinary Medicine, Columbia University. Tumor watch studies were conducted on animals in a mixed (Sv129xC57/BL6) background (i.e., the second and third backcross generations for the line 4E12 and the first and second backcross generation for the lines 5H7 and 4B8). Within each line, comparable numbers of age-matched wt littermates controlled for possible differences in lymphoma incidence. Animals were monitored for a minimum of 18 months and a subgroup analyzed every 6 months for the presence of abnormalities. Mice that survived the duration of the study were sacrificed, and a necropsy was performed. When possible, necropsies were performed on dead animals to determine whether they had gross evidence of tumors. Statistical analysis was performed on the Statview program (SAS Institute Inc., Cary, NC) using Kaplan-Meier cumulative survival and the log-rank (Mantel-Cox) test to determine whether differences were significant. The χ^2 test was used to compare B-NHL incidence in IμHABCL6 knockin mice versus wt littermates.

Mice immunization

For analysis of T cell-dependent immune responses, age- and sex-matched mice were immunized intraperitoneally at ~8 weeks of age with 0.5 ml of a 2% SRBC suspension in PBS (Cocalico Biologicals, PA), and sacrificed after 10 days. For tumor development survey, a cohort of animals was kept under repeated antigenic stimulation by injecting SRBC every 3 weeks until death or tumor development.

Northern blot and Western blot analysis

CD19$^+$ and CD19$^-$ splenic B cells were isolated by a magnetic cell separation protocol using MACS columns (Miltenyi Biotech, Auburn, CA). Total RNA was extracted from thymus, CD19$^+$, and CD19$^-$ B cells using the Trizol reagent (Invitrogen Life Technologies, Carlsbad, CA), and Northern blot analysis for BCL6 expression was performed as described (Cattoretti et al., 1995). Total protein extracts were prepared from the above cell populations using RIPA buffer, gel electrophoresed on 4%–12% gradient SDS/PAGE gels (Invitrogen), transferred to nitrocellulose membranes (Sheller & Schuell), and immunostained according to standard methods using anti-BCL6 (N3) rabbit polyclonal Abs (Santa Cruz Biotechnology, Santa Cruz, CA), anti-HA rat monoclonal Abs (Covance, Princeton, NJ), and an anti-β actin Ab (AC15, Sigma, St. Louis, MO) as control for loading (Cattoretti et al., 1995). Proteins were detected using the ECL reagents (Amersham Biosciences) as recommended by the manufacturer.

Flow cytometry

The following antibody combinations were used on single cell suspensions from normal organs or tumors: A: B220, IgM, IgD, Ig kappa light chain; B: B220, CD23, CD21, CD11b; C: IgM, CD43, CD5, CD19; D: B220, CD138, IgM, IgD, Ig kappa light chain; E: B220, CD69, CD80; F: B220, A44.1, IgM, CD43; G: CD3, CD4, CD8. The enumeration of GC-type of cells was performed by four-color staining with B220, PNA, CD38, and GL7. All antibodies were from BD Pharmingen (San Diego, CA), except for the IgD-Pe (Southern Biotechnology Inc., Birmingham, AL). Data were acquired on a FACSCalibur (Becton Dickinson) and analyzed with CELLQuest software.

Histology, immunohistochemistry, and immunofluorescence

Four μm-thick formalin-fixed, paraffin-embedded sections were stained for H&E or immunostained as published previously (Ye et al., 1997), using the following primary antibodies: rabbit anti-BCL6 (N3), goat anti-IRF4, goat

anti-Pax5, mouse IgG1 anti Pax5 (Santa Cruz Biotechnology, Santa Cruz, CA), donkey anti IgM (Jackson Immunoresearch Laboratories, West Grove, PA), mouse IgG1 anti BCL6 (Novocastra Laboratories, Newcastle upon Tyne, UK), rat anti B220, CD138 (BD Pharmingen), HA (Roche Applied Sciences, Indianapolis, IN), PNA lectin (Vector, Burlingame, CA). Double immunohistochemical stainings were performed as published previously (Cattoretti et al., 1995) with noncrossreacting combinations of primary and secondary antibodies.

Somatic hypermutation analysis

Genomic DNA was isolated from tumor specimens by the salting-out method, and the rearranged VH sequences were amplified by PCR, using forward primers that anneal to the framework region III of the most abundantly used VH J558 family or to the VH7183 family, and reverse primers positioned in the JH3 or JH4 intron in separate reactions (Jolly et al., 1997). PCR conditions were 94°C for 30 s, 63°C for 30 s and 72°C for 2 min, for 35 cycles. Using this protocol, a polyclonal B cell population can be detected as three major PCR fragments (four if the reverse JH4 primer is used), corresponding to cells where the JH1, JH2, JH3 (and JH4) segments were rearranged. Conversely, a clonal population (e.g., a tumor) gives either a unique band (the tumor clone) or a predominant band over a faint background (residual nontumor cells in the sample). PCR products were gel-purified using the QIAQUICK purification method (QIAGEN) and sequenced directly on a ABI377 sequencer. Sequences were compared to the NCBI databases and to our own database to rule out polymorphisms as well as contamination with previously amplified rearrangements.

SKY

Multicolor spectral karyotyping was performed on representative spleen and tumor specimens according to standard procedures (Harris et al., 2003).

Supplemental data

Supplemental data for this article can be found at http://www.cancercell.org/cgi/content/full/7/5/445/DC1/.

Acknowledgments

We thank U. Klein for discussions, R. Baer for critically reading the manuscript, D. Washton for excellent technical help, and L. Yang and the Molecular Pathology Facility of the Herbert Irving Cancer Center at Columbia University Medical Center for histology service. We also thank Dr. T. Honjo for the AID$^{-/-}$ mice. J. Gerdes (Molecular Immunology, Borstel, DRG) generously provided the rabbit anti-mouse Ki-67 antibodies. L.P. is a Special Fellow of the Leukemia & Lymphoma Society. This work is supported by NIH grant CA092625.

Received: November 26, 2004
Revised: February 13, 2005
Accepted: March 24, 2005
Published: May 16, 2005

References

Baron, B.W., Anastasi, J., Montag, A., Huo, D., Baron, R.M., Karrison, T., Thirman, M.J., Subudhi, S.K., Chin, R.K., Felsher, D.W., et al. (2004). The human BCL6 transgene promotes the development of lymphomas in the mouse. Proc. Natl. Acad. Sci. USA *101*, 14198–14203.

Bereshchenko, O.R., Gu, W., and Dalla-Favera, R. (2002). Acetylation inactivates the transcriptional repressor BCL6. Nat. Genet. *32*, 606–613.

Capello, D., Vitolo, U., Pasqualucci, L., Quattrone, S., Migliaretti, G., Fassone, L., Ariatti, C., Vivenza, D., Gloghini, A., Pastore, C., et al. (2000). Distribution and pattern of BCL-6 mutations throughout the spectrum of B-cell neoplasia. Blood *95*, 651–659.

Cattoretti, G., Chang, C.C., Cechova, K., Zhang, J., Ye, B.H., Falini, B., Louie, D.C., Offit, K., Chaganti, R.S., and Dalla-Favera, R. (1995). BCL-6 protein is expressed in germinal-center B cells. Blood *86*, 45–53.

Chang, C.C., Ye, B.H., Chaganti, R.S., and Dalla-Favera, R. (1996). BCL-6, a POZ/zinc-finger protein, is a sequence-specific transcriptional repressor. Proc. Natl. Acad. Sci. USA *93*, 6947–6952.

Chen, W., Iida, S., Louie, D.C., Dalla-Favera, R., and Chaganti, R.S. (1998). Heterologous promoters fused to BCL6 by chromosomal translocations affecting band 3q27 cause its deregulated expression during B-cell differentiation. Blood *91*, 603–607.

Dalla-Favera, R., and Gaidano, G. (2001). Molecular Biology of Lymphomas. In Cancer, Principles and Practice of Oncology., V.T. De Vita, S. Hellman, and S.A. Rosenberg, eds. (Philadelphia: Lippincott Williams & Wilkins), pp. 2215–2235.

Dent, A.L., Shaffer, A.L., Yu, X., Allman, D., and Staudt, L.M. (1997). Control of inflammation, cytokine expression, and germinal center formation by BCL-6. Science *276*, 589–592.

Falini, B., Fizzotti, M., Pucciarini, A., Bigerna, B., Marafioti, T., Gambacorta, M., Pacini, R., Alunni, C., Natali-Tanci, L., Ugolini, B., et al. (2000). A monoclonal antibody (MUM1p) detects expression of the MUM1/IRF4 protein in a subset of germinal center B cells, plasma cells, and activated T cells. Blood *95*, 2084–2092.

Fujita, N., Jaye, D.L., Geigerman, C., Akyildiz, A., Mooney, M.R., Boss, J.M., and Wade, P.A. (2004). MTA3 and the Mi-2/NuRD complex regulate cell fate during B lymphocyte differentiation. Cell *119*, 75–86.

Harris, M.B., Chang, C.C., Berton, M.T., Danial, N.N., Zhang, J., Kuehner, D., Ye, B.H., Kvatyuk, M., Pandolfi, P.P., Cattoretti, G., et al. (1999). Transcriptional repression of Stat6-dependent interleukin-4-induced genes by BCL-6: Specific regulation of i epsilon transcription and immunoglobulin E switching. Mol. Cell. Biol. *19*, 7264–7275.

Harris, C.P., Lu, X.Y., Narayan, G., Singh, B., Murty, V.V., and Rao, P.H. (2003). Comprehensive molecular cytogenetic characterization of cervical cancer cell lines. Genes Chromosomes Cancer *36*, 233–241.

Hoyer, K.K., French, S.W., Turner, D.E., Nguyen, M.T., Renard, M., Malone, C.S., Knoetig, S., Qi, C.F., Su, T.T., Cheroutre, H., et al. (2002). Dysregulated TCL1 promotes multiple classes of mature B cell lymphoma. Proc. Natl. Acad. Sci. USA *99*, 14392–14397.

Jolly, C.J., Klix, N., and Neuberger, M.S. (1997). Rapid methods for the analysis of immunoglobulin gene hypermutation: Application to transgenic and gene targeted mice. Nucleic Acids Res. *25*, 1913–1919.

Kerckaert, J.P., Deweindt, C., Tilly, H., Quief, S., Lecocq, G., and Bastard, C. (1993). LAZ3, a novel zinc-finger encoding gene, is disrupted by recurring chromosome 3q27 translocations in human lymphomas. Nat. Genet. *5*, 66–70.

Küppers, R., and Dalla-Favera, R. (2001). Mechanisms of chromosomal translocation in B-cell lymphoma. Oncogene *20*, 5580–5594.

Küppers, R., Klein, U., Hansmann, M.L., and Rajewsky, K. (1999). Cellular origin of human B-cell lymphomas. N. Engl. J. Med. *341*, 1520–1529.

Lennon, G.G., and Perry, R.P. (1985). C mu-containing transcripts initiate heterogeneously within the IgH enhancer region and contain a novel 5′-nontranslatable exon. Nature *318*, 475–478.

Li, S.C., Rothman, P.B., Zhang, J., Chan, C., Hirsh, D., and Alt, F.W. (1994). Expression of I mu-C gamma hybrid germline transcripts subsequent to immunoglobulin heavy chain class switching. Int. Immunol. *6*, 491–497.

Lin, K.I., Tunyaplin, C., and Calame, K. (2003). Transcriptional regulatory cascades controlling plasma cell differentiation. Immunol. Rev. *194*, 19–28.

Lo Coco, F., Ye, B.H., Lista, F., Corradini, P., Offit, K., Knowles, D.M., Chaganti, R.S., and Dalla-Favera, R. (1994). Rearrangements of the BCL6 gene in diffuse large cell non-Hodgkin's lymphoma. Blood *83*, 1757–1759.

Migliazza, A., Martinotti, S., Chen, W., Fusco, C., Ye, B.H., Knowles, D.M., Offit, K., Chaganti, R.S., and Dalla-Favera, R. (1995). Frequent somatic hypermutation of the 5′ noncoding region of the BCL6 gene in B-cell lymphoma. Proc. Natl. Acad. Sci. USA *92*, 12520–12524.

Muramatsu, M., Kinoshita, K., Fagarasan, S., Yamada, S., Shinkai, Y., and

Honjo, T. (2000). Class switch recombination and hypermutation require activation-induced cytidine deaminase (AID), a potential RNA editing enzyme. Cell *102*, 553–563.

Niu, H., Ye, B.H., and Dalla-Favera, R. (1998). Antigen receptor signaling induces MAP kinase-mediated phosphorylation and degradation of the BCL-6 transcription factor. Genes Dev. *12*, 1953–1961.

Niu, H., Cattoretti, G., and Dalla-Favera, R. (2003). BCL6 controls the expression of the B7–1/CD80 costimulatory receptor in germinal center B cells. J. Exp. Med. *198*, 211–221.

Pasqualucci, L., Migliazza, A., Fracchiolla, N., William, C., Neri, A., Baldini, L., Chaganti, R.S., Klein, U., Küppers, R., Rajewsky, K., and Dalla-Favera, R. (1998). BCL-6 mutations in normal germinal center B cells: Evidence of somatic hypermutation acting outside Ig loci. Proc. Natl. Acad. Sci. USA *95*, 11816–11821.

Pasqualucci, L., Bereschenko, O., Niu, H., Klein, U., Basso, K., Guglielmino, R., Cattoretti, G., and Dalla-Favera, R. *Suppl 3*(2003a). Molecular pathogenesis of non-Hodgkin's lymphoma: The role of Bcl-6. Leuk. Lymphoma *44*, S5–12.

Pasqualucci, L., Migliazza, A., Basso, K., Houldsworth, J., Chaganti, R.S., and Dalla-Favera, R. (2003b). Mutations of the BCL6 proto-oncogene disrupt its negative autoregulation in diffuse large B-cell lymphoma. Blood *101*, 2914–2923.

Peng, H.Z., Du, M.Q., Koulis, A., Aiello, A., Dogan, A., Pan, L.X., and Isaacson, P.G. (1999). Nonimmunoglobulin gene hypermutation in germinal center B cells. Blood *93*, 2167–2172.

Phan, R.T., and Dalla-Favera, R. (2004). The BCL6 proto-oncogene suppresses p53 expression in germinal-centre B cells. Nature *432*, 635–639.

Polo, J.M., Dell'Oso, T., Ranuncolo, S.M., Cerchietti, L., Beck, D., Da Silva, G.F., Prive, G.G., Licht, J.D., and Melnick, A. (2004). Specific peptide interference reveals BCL6 transcriptional and oncogenic mechanisms in B-cell lymphoma cells. Nat. Med. *10*, 1329–1335.

Rajewsky, K. (1996). Clonal selection and learning in the antibody system. Nature *381*, 751–758.

Ranger, A.M., Zha, J., Harada, H., Datta, S.R., Danial, N.N., Gilmore, A.P., Kutok, J.L., Le Beau, M.M., Greenberg, M.E., and Korsmeyer, S.J. (2003). Bad-deficient mice develop diffuse large B cell lymphoma. Proc. Natl. Acad. Sci. USA *100*, 9324–9329.

Reljic, R., Wagner, S.D., Peakman, L.J., and Fearon, D.T. (2000). Suppression of signal transducer and activator of transcription 3-dependent B lymphocyte terminal differentiation by BCL-6. J. Exp. Med. *192*, 1841–1848.

Seyfert, V.L., Allman, D., He, Y., and Staudt, L.M. (1996). Transcriptional repression by the proto-oncogene BCL-6. Oncogene *12*, 2331–2342.

Shaffer, A.L., Yu, X., He, Y., Boldrick, J., Chan, E.P., and Staudt, L.M. (2000). BCL-6 represses genes that function in lymphocyte differentiation, inflammation, and cell cycle control. Immunity *13*, 199–212.

Shaffer, A.L., Lin, K.I., Kuo, T.C., Yu, X., Hurt, E.M., Rosenwald, A., Giltnane, J.M., Yang, L., Zhao, H., Calame, K., and Staudt, L.M. (2002). Blimp-1 orchestrates plasma cell differentiation by extinguishing the mature B cell gene expression program. Immunity *17*, 51–62.

Shen, H.M., Peters, A., Baron, B., Zhu, X., and Storb, U. (1998). Mutation of BCL-6 gene in normal B cells by the process of somatic hypermutation of Ig genes. Science *280*, 1750–1752.

Stavnezer, J., Sirlin, S., and Abbott, J. (1985). Induction of immunoglobulin isotype switching in cultured I.29 B lymphoma cells. Characterization of the accompanying rearrangements of heavy chain genes. J. Exp. Med. *161*, 577–601.

Tunyaplin, C., Shaffer, A.L., Angelin-Duclos, C.D., Yu, X., Staudt, L.M., and Calame, K.L. (2004). Direct repression of prdm1 by Bcl-6 inhibits plasmacytic differentiation. J. Immunol. *173*, 1158–1165.

Wang, X., Li, Z., Naganuma, A., and Ye, B.H. (2002). Negative autoregulation of BCL-6 is bypassed by genetic alterations in diffuse large B cell lymphomas. Proc. Natl. Acad. Sci. USA *99*, 15018–15023.

Ye, B.H., Lista, F., Lo Coco, F., Knowles, D.M., Offit, K., Chaganti, R.S., and Dalla-Favera, R. (1993a). Alterations of a zinc finger-encoding gene, BCL-6, in diffuse large-cell lymphoma. Science *262*, 747–750.

Ye, B.H., Rao, P.H., Chaganti, R.S., and Dalla-Favera, R. (1993b). Cloning of bcl-6, the locus involved in chromosome translocations affecting band 3q27 in B-cell lymphoma. Cancer Res. *53*, 2732–2735.

Ye, B.H., Chaganti, S., Chang, C.C., Niu, H., Corradini, P., Chaganti, R.S., and Dalla-Favera, R. (1995). Chromosomal translocations cause deregulated BCL6 expression by promoter substitution in B cell lymphoma. EMBO J. *14*, 6209–6217.

Ye, B.H., Cattoretti, G., Shen, Q., Zhang, J., Hawe, N., de Waard, R., Leung, C., Nouri-Shirazi, M., Orazi, A., Chaganti, R.S., et al. (1997). The BCL-6 proto-oncogene controls germinal-centre formation and Th2-type inflammation. Nat. Genet. *16*, 161–170.